Solar Energy 163 (2018) 434–442

Contents lists available at ScienceDirect

Solar Energy

journal homepage: www.elsevier.com/locate/solener

Pentacene-assisted planarization of photo-active layers for high performance tandem organic photovoltaics

Feng Yang[a], Dong-Won Kang[b,*], Yong-Sang Kim[a,*]

[a] School of Electronic and Electrical Engineering, Sungkyunkwan University, Suwon, Gyeonggi 16419, Republic of Korea
[b] School of Energy Systems Engineering, Chung-Ang University, Seoul 06974, Republic of Korea

ARTICLE INFO

Keywords:
Tandem organic solar cells
Organic photovoltaics
Pentacene
High temperature annealing

ABSTRACT

In organic tandem solar cells, the morphology of the photo-active layers is not usually stable when their fabrication processes are made with several thermal treatments. Here, we report pentacene-assisted planar tandem organic photovoltaic device based on the active layers of poly(3-hexylthiophene) (P3HT) and (6,6)-phenyl C61-butyric acid methyl ester (PCBM), fabricated in air-ambient. An additive of pentacene was introduced into the active layers of the bottom sub-cells for planarization on their surfaces. The surface morphology of pentacene-based active layer was maintained to be flat from 80 to 160 °C, and allowed for fabricating the planar active layers and interconnecting layer of tandem devices against thermal treatment. State-of-the-art homo-tandem organic solar cells were achieved with an average power conversion efficiency (PCE) of 3.5%, while their best single junction solar cells of P3HT:PCBM achieved a PCE of 3.2%. We showed the first application of high performance tandem organic photovoltaics with three times of high temperature annealing processes at 160 °C. Our work demonstrates a practical way to design highly efficient tandem organic solar cells with other powerful and well-chosen bandgap energy active layers during thermal treatments.

1. Introduction

The power conversion efficiency (PCE) of organic photovoltaics (OPVs) has been highly developed by more than 10% (Cheng et al., 2016; Ouyang et al., 2015; You et al., 2013). For higher PCE, tandem organic solar cells have attracted enormous research interest to harvest more solar energy. Recently, many papers report more than 12% PCE of tandem OPV devices (Li et al., 2017; Zhang, K. et al., 2016; Zhang, Q. et al., 2016), and the highest PCE is to date 13.8% (Cui et al., 2017). However, a theoretical maximum PCE of 40% for tandem photovoltaics is proposed by employing well-chosen bandgap energies for their active layers (Rabady and Manasreh, 2017). Thus, there is much room to improve the performance of tandem organic solar cells.

There are a lot of technologies to develop the performance of tandem OPVs, such as the synthesis of new organic materials for active layers (Dou et al., 2012; Li et al., 2016), and various designs of interconnection layer (ICL) (Ameri et al., 2013; Etxebarria et al., 2015). ICL is a very critical connector between the sub-cells of tandem devices. For an ICL, it typically consists of a hole transport layer (HTL) and an electron transport layer (ETL). Solution-processed HTLs or ETLs for ICLs are very popular approaches, such as poly(3,4-ethylenedioxythiophene): poly-styrene sulfonate (PEDOT:PSS) (Chen et al., 2014, 2013), MoO_x (Lu et al., 2015), ZnO (Kouijzer et al., 2012), or TiO_x (Kong et al., 2012; Yang et al., 2011). Some HTLs or ETLs of metal oxide nanoparticles are processed at room-temperature (Lu et al., 2015; Zhou et al., 2015). However, the layers of metal oxide nanoparticles are not robust enough for ICLs, which typically need another very thick sub-layer of ICLs to protect the underlying sub-cells from the solvents of the later processes. The thick extra sub-layer of ICLs would increase their resistance and light absorption, and decrease the PCE of tandem solar cells (Chen et al., 2015). Usually, solution-processed HTLs or ETLs prefer some thermal treatment at about 100–300 °C (Wang, K. et al., 2016). Thermally treated ICLs would be more robust and efficient for tandem devices (Yang et al., 2017a). Moreover, thermal treatment on the organic single junction solar cells significantly improved their PCE performance (Busireddy et al., 2016; Proudian et al., 2016; Wang, J.L. et al., 2016). Hence, it is highly interesting to fabricate tandem organic solar cells with thermal treatment processes.

In order to fabricate the tandem OPV devices against thermal processing, morphologically-stable bottom sub-cells under the thermal processing are very fundamental to the ICL and top sub-cells of tandem devices. Under high temperature annealing, the acceptor in the active layer of OPVs devices, typical fullerene derivative [6,6]-phenyl-C61-butyric acid methyl ester (PCBM), emerges and aggregates into

* Corresponding authors.
E-mail addresses: kangdwn@cau.ac.kr (D.-W. Kang), yongsang@skku.edu (Y.-S. Kim).

https://doi.org/10.1016/j.solener.2018.01.093
Received 14 November 2017; Received in revised form 26 January 2018; Accepted 31 January 2018

micrometer-sized crystals on the surface of active layer (Ben Dkhil et al., 2017; Salim et al., 2016), and usually leads to defects or failure of fabrication of ICL and top sub-cell. Some studies tried to fabricate thermally stable active layers for organic single-junction solar cells, such as cross-linking of the polymer (Kim et al., 2012) or fullerene (Hsieh et al., 2010), and introducing additive molecules (Grant et al., 2017; Wang et al., 2015; Yang et al., 2015). We found that there are no papers reporting tandem organic solar cells with several thermal annealing processes at high temperature. The harsh high temperature up to 150 °C may ruin the morphology of the underlying active layer, so that Chen et al. just applied at mild post-treatment of 80 °C on the ICL of their tandem OPVs (Chen et al., 2017). In particular for a top sub-cell of tandem OPVs, the active layer was mostly fabricated with solvent annealing (Li et al., 2017) or additive treatment (Cui et al., 2017), which avoids any thermal impact on the performance of tandem devices. The performance of additive treated OPV devices strongly decreased under thermal stress (Ben Dkhil et al., 2017). In any event, it is very hard to apply them to the industrial manufacturing process, which always involves many thermal processes (Jørgensen et al., 2012). In our previous study (Yang et al., 2015), organic single-junction solar cells with the additive of pentacene were thermally stable for 24 h at 120 °C, and kept 70% of their original PCE. The surface of their active layer has few micrometer-sized crystals of PCBM after the thermal treatment. Hence, for fabricating the planar ICL and top sub-cell of tandem OPVs with multi-thermal treatment, there is a chance of a bottom sub-cell with morphological engineering of pentacene.

In this work, we developed the first application of efficient tandem organic solar cells with three times of high temperature annealing processes at 160 °C. The tandem OPV device structure and chemical structures of organic materials for active layers are shown in Fig. 1(a) and (b). The sub-cell with morphology engineering of pentacene was deeply studied from 80 to 160 °C. The planar tandem organic solar cells based on the P3HT:PCBM system achieved an average PCE of 3.54% with short-circuit current density (J_{SC}) = 4.79 mA/cm^2, open-circuit voltage (V_{OC}) = 1.18 V, and fill factor (FF) = 0.63. The PCE of tandem devices with 160 °C annealing is much comparable to the recently published homo-tandem OPVs based on the P3HT:PCBM system of 3.2–3.5% with 100 °C annealing (Lu et al., 2016, 2015).

2. Experimental section

2.1. Device fabrication

Poly(3-hexylthiophene) (P3HT) (from Rieke Metals), [6,6]-Phenyl C61 butyric acid methyl ester (PCBM) (from Nano-C) and pentacene (from Polysis Company) were used as received without further treatment. A PEDOT:PSS solution (Clevious PVP AI 4083) was modified with Triton X-100 (0.5% v/v). For single-junction cell, patterned ITO substrates were ultra-sonicated sequentially in deionized water, acetone, and then isopropyl alcohol for 20 min of each step. A ZnO layer (ca. 40 nm) was prepared on the ITO substrate (Yang et al., 2015). P3HT:PCBM:pentacene (1:1:0.2 w/w) for the active layers of various thicknesses, dissolved in chlorobenzene by ultra-sonication, was spin-coated on the ZnO layers. The modified PEDOT:PSS solution was spin-coated on the active layers, and thermally treated at 160 °C for 10 min (Yang et al., 2016). A silver (Ag) electrode (ca. 100 nm) was deposited on the PEDOT layer by a thermal evaporator. For tandem solar cells, an inter-connecting layer (ICL) of MoO_3/Au/Al/ZnO layer was deposited on the bottom sub-cells as our previous study (Yang et al., 2017a). The wet ZnO film of ICL was thermally treated at 160 °C for 10 min. The active layer, PEDOT:PSS, and Ag layer of top sub-cells were fabricated similarly as the single-junction solar cells procedure. All fabrication of single-junction cells and tandem solar cells were fabricated in the ambient air (20–40% relative humidity) except the thermal evaporation processes. The area of all cells was 0.09 cm^2, defined by the overlap area between the ITO and the Ag electrode.

2.2. Device characterization

The scanning electron microscope (SEM) images were obtained with a JEOL JSM7000F field emission scanning electron microscope (FESEM). All SEM samples were applied platinum-coating prior to SEM imaging. Atomic force microscopy (AFM) images were measured with an advanced scanning probe microscope (PSIA Corp.). The thicknesses of active layers were characterized from the average values of their AFM images. Optical microscopy images were acquired by an Olympus BX41 Microscope Digital Camera. The current density – voltage (J–V) characterization of solar cells was measured with a J-V curve tracer

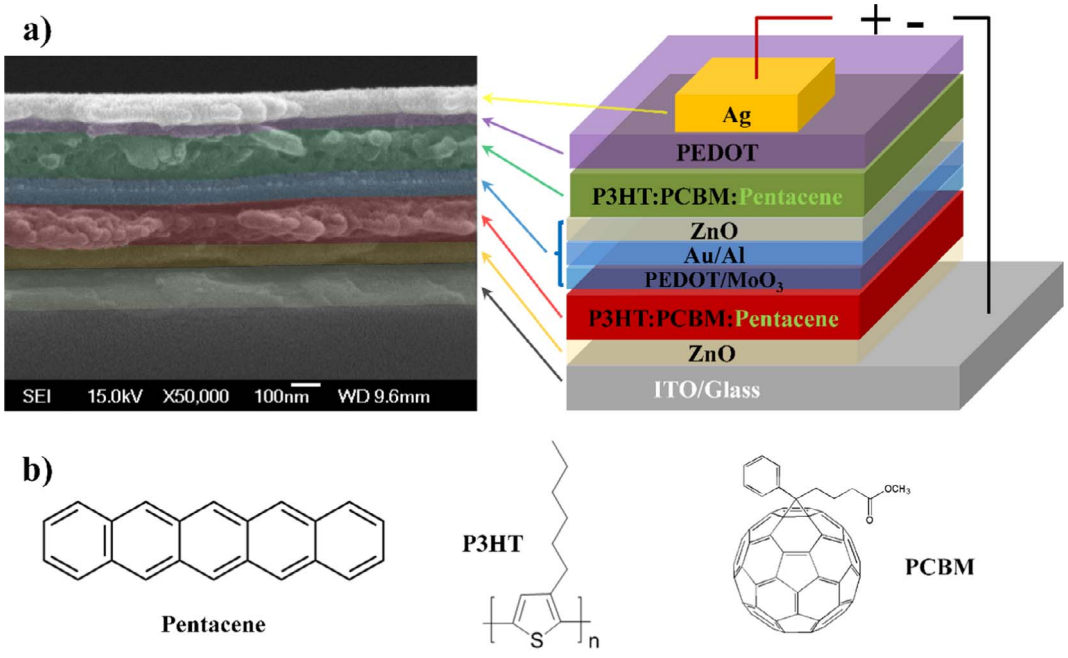

Fig. 1. (a) The cross-section SEM image (false color) and device structure of tandem OPVs: ITO/ZnO/P3HT:PCBM:Pentacene/PEDOT:PSS/MoO_3/Au/Al/ZnO/P3HT:PCBM:Pentacene/PEDOT:PSS/Ag. (b) Chemical structures of pentacene, P3HT, and PCBM in tandem OPV cells.

(Eko MP-160) and a solar simulator (Yss-E40, Yamashita Denso) under AM 1.5G irradiation (100 mW/cm^2), calibrated by Newport certified standard silicon cell. The UV–vis absorption and transmittance spectra were obtained by a Shimadzu UV-1601 UV–Vis spectrophotometer. The external quantum efficiency (EQE) was measured on a solar cell IPCE measurement system K3100 EQX (McScience Inc.).

3. Results and discussion

In this study, we fabricated the inverted tandem organic solar cells with multi-thermal treatment at 160 °C. Fig. S1 (supplementary information) and Fig. 1(a) show their energy level diagram and device structure. The bottom and top sub-cells were both fabricated with thermal annealing at 160 °C for 10 min. The charge recombination ICL of MoO_3/Au/Al/ZnO was deposited similarly as our previous study (Yang et al., 2017a), and the ZnO film of the ICL was also under thermal treatment at 160 °C for 10 min. Thus, three processes of thermal treatment at 160 °C were applied during the fabrication process of the tandem OPV devices. Morphological engineering of active layers with pentacene would make tandem organic solar cells planar and stable against the thermal processes, as shown in Fig. 1(a).

The active layer in bottom sub-cells is the key issue for the tandem OPVs under the high temperature of 160 °C. The thermal property of the active layer was extensively studied. Fig. 2(a) shows the single cell used for the tandem device, ITO/ZnO/P3HT:PCBM:pentacene/PEDOT:PSS/Ag. We found that the performance of the single cell is very sensitive to the thermal annealing temperature. Fig. 2(b) shows that when the annealing temperature for active layer increased from 80 to 160 °C, the J_{SC} increased from 3.29 to 6.64 mA/cm^2. Meanwhile, when the active layer thickness increased from 90 to 170 nm with keeping thermal-annealing at 160 °C, the J_{SC} increased from 6.64 mA/cm^2 to 9.17 mA/cm^2. Thus, when the thickness increases, the PCE of a single cell increases, as shown in Fig. 2(c). When the thickness of the active layer is more than 130 nm, the PCE and FF decrease (in Fig. 2(d)), because a thicker active layer is not good for the charge extraction, and increases the charge recombination inside of the active layer. The V_{OC} of single cells did not change much with different thickness. These various thicknesses of single cells are very useful to balance the current matching in the tandem organic solar cells.

Surface engineering should be applied on the bottom sub-cells of tandem OPVs since the PCBM crystallites can grow easily on the surface of the active layer under the thermal annealing process (Berriman et al., 2016; Li et al., 2016; Watts et al., 2009). Some papers have confirmed the PCBM crystallites on the surface by EDS spectral analysis of elemental distribution (Akogwu et al., 2011), and selected-area-electron-diffraction transmission-electron-microscopy (Mon et al., 2015). In order to modify the active layer with planar surface, we introduced pentacene into the active layer to suppress the crystallization of PCBM. Pentacene could easily bond with PCBM molecules because of many π-electrons on their molecule surfaces. Fig. 3 shows a schematic of the crystallization process of PCBM in the active layer and the suppressing effect of pentacene under thermal annealing. Before thermal treatment, the P3HT and PCBM are randomly located in the active layer. When the pentacene is involved in the P3HT:PCBM blend, the π-π interaction between the PCBM and pentacene weakens the interaction of PCBM molecules (Yang et al., 2015). Then, the PCBM molecules, bonded with pentacene, could not easily aggregate under a thermal annealing process. Fig. 3(a) shows that the PCBM crystals emerge on the surface of active layer without pentacene under thermal annealing. As a result, the crystallites of PCBM grow on the surface layer and ruin the planar morphology of active layer. Fig. 3(b) shows that on the other hand, the motion of PCBM molecules with pentacene is very limited. During a

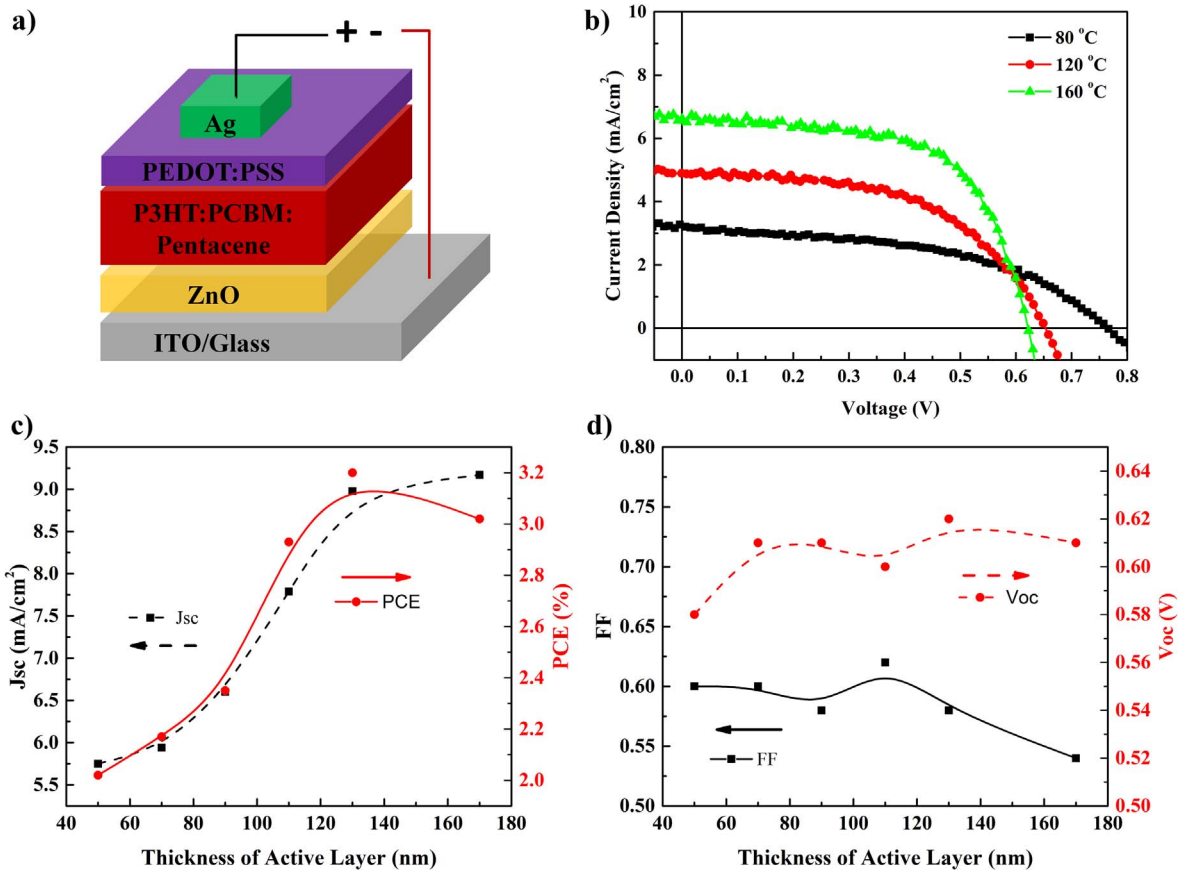

Fig. 2. (a) Device structure of single-junction cells. (b) Current density – voltage (*J–V*) characteristics of single-junction cell with annealed active layer at 80 °C, 120 °C, and 160 °C. Single-junction cell performance of (c) PCE and J_{SC}, and (d) FF and V_{OC}, with various thicknesses of active layer.

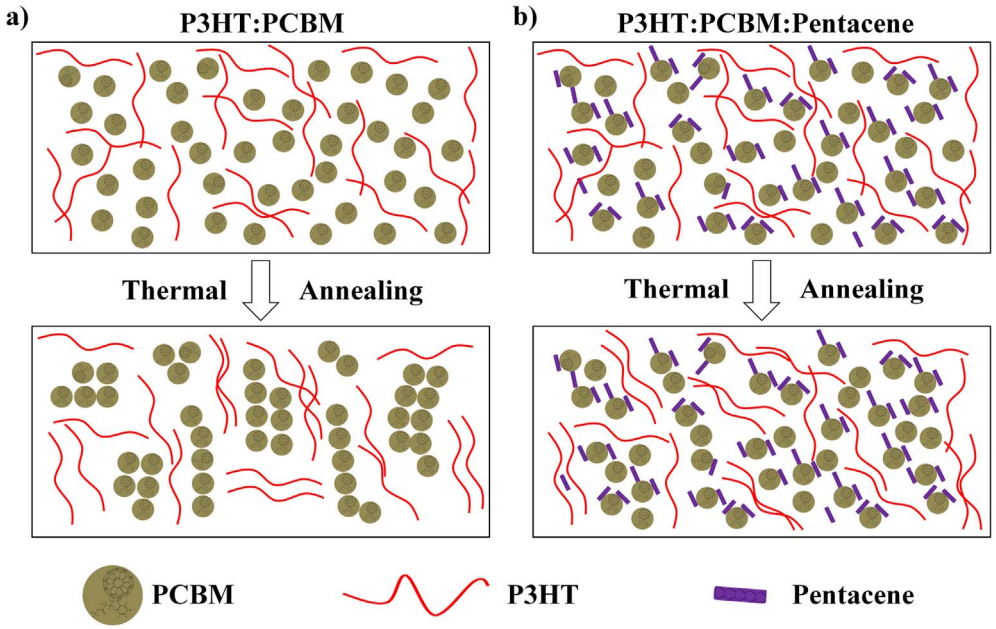

Fig. 3. Schematic representation of (a) the crystallization process of PCBM in the active layer, and (b) the suppressing effect of pentacene on its nucleation process under thermal treatment.

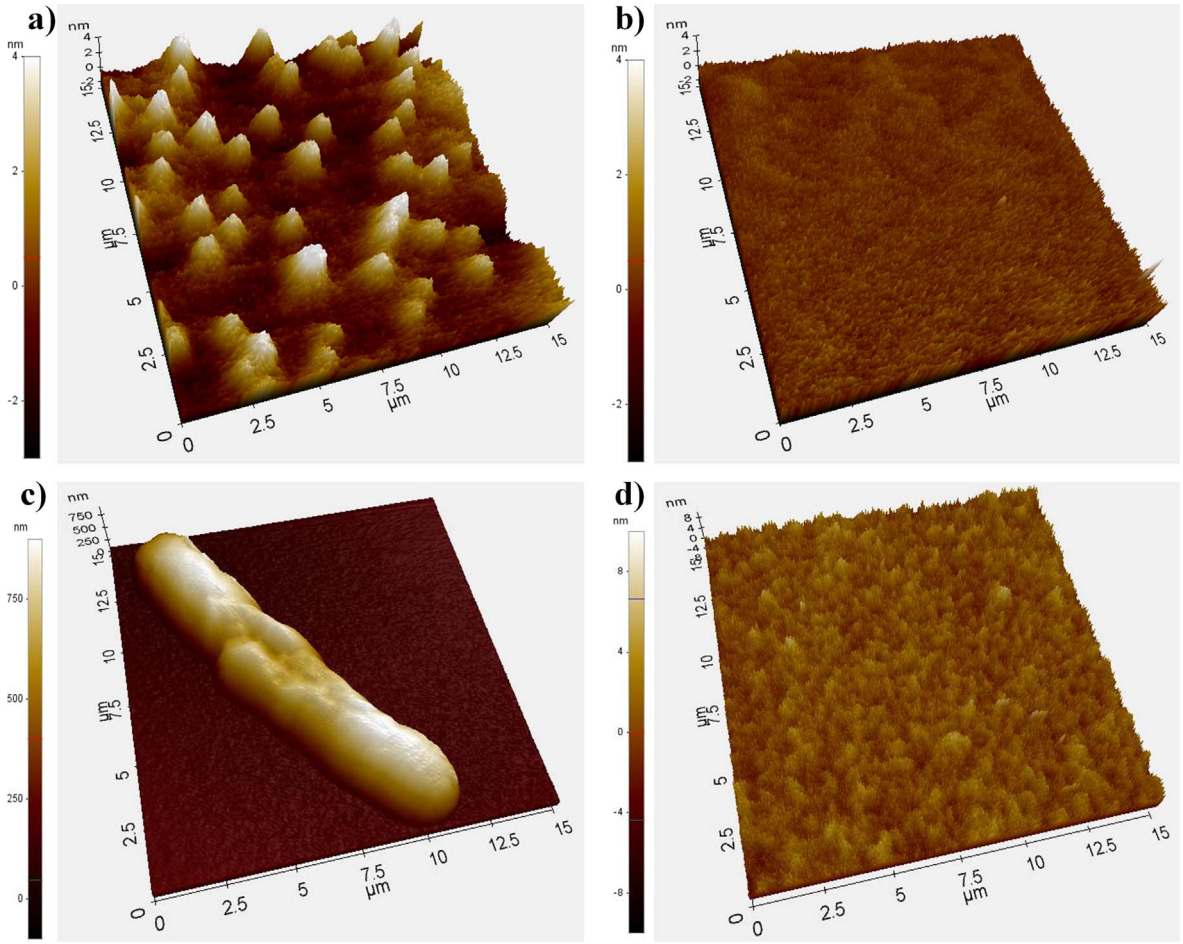

Fig. 4. Atomic force microscopy topography 3D images of active layer (a) P3HT:PCBM, and (b) P3HT:PCBM:Pentacene, annealed at 80 °C for 1 h; (c) P3HT:PCBM, and (d) P3HT:PCBM:Pentacene, annealed at 160 °C for 10 min. The size of all images is 15 μm × 15 μm.

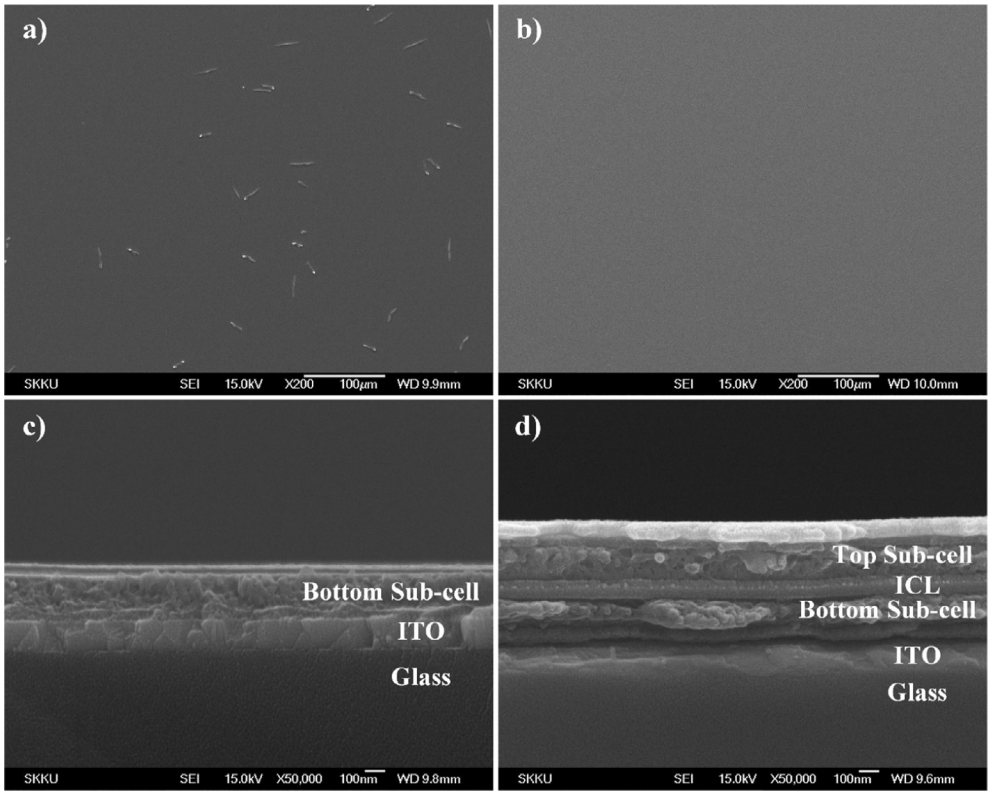

Fig. 5. SEM images of the active layer surfaces of single cells modified (a) without pentacene, and (b) with pentacene after thermal treatment of 160 °C. The cross-section SEM images of (c) bottom sub-cell and (d) tandem OPV cells modified with pentacene.

thermal annealing process, it is very hard for pentacene-PCBM molecule to diffuse or move together, which results in a planar surface of the active layer.

The pentacene-assisted planarization of the active layer is clearly evident in the AFM images (Fig. 4) and SEM images (Fig. 5(a) and (b)) of the active layers with and without pentacene. Fig. 4(a) shows that small crystallites of PCBM formed on the surface, of 1–2 μm length and 2–4 nm height, even though the active layer was annealed at 80 °C. However, Fig. 4(b) shows that there were no PCBM crystallites on the surface of the active layer with pentacene. Fig. 4(c) shows that with a higher annealing temperature (160 °C), a PCBM crystal on the surface of the active layer without pentacene is much clearer. On the other hand, Fig. 4(d) shows that the active layer with pentacene has a planar morphology. When the thermal annealing temperature increases from 80 to 160 °C, the size of PCBM crystals increases from 1 to 2 μm to tens of μm in length, and from 2 to 4 nm to hundreds of nm in height; whereas, the active layer with pentacene has a flat and planar surface. The PCBM crystals were also clearly found, and tens of μm in length from the SEM images in Fig. 5(a). Fig. 5(b) shows that the very planar morphology of active layer with the morphological engineering of pentacene was obtained. As a result, the planar bottom sub-cell, interconnecting layer and tandem OPV device was fabricated as showed in Fig. 5(c) and (d). Hence, the PCBM crystals are considered a severe problem for the fabrication of sub-cells and ICL of tandem OPV devices, since their thickness (hundreds of nm) is much larger than the thickness of the ICL (tens of nm) and the top sub-cell (ca. 100 nm), and easily leads to defects in the ICL and sub-cells.

The planar morphology of active layer is further studied by microscopy images (Fig. 6). In Fig. 6(b) and (d), there are no PCBM crystallites on the surface of the active layer with pentacene under thermal treatment at 120 or 160 °C. Fig. 6(a) shows that with annealing temperature of 120 °C, the crystallization of PCBM on the surface of the active layer without pentacene is much clearer. Fig. 6(c) shows that their sizes are increased in length with a higher temperature of 160 °C. The size of PCBM crystallites on the active layer without pentacene reaches over 100 μm in length (Fig. 6(c)), and a few hundred nm in thickness (Fig. 6(e)). On the basis of the active layer, ICLs of the tandem devices were constructed on their sub-cells (Fig. S2 of the supplementary information). Fig. 6(f) shows that the ICL on the surface of active layer without pentacene had defects on the top of ICL over the PCBM crystals, which is a severe problem for the fabrication of ICL for tandem OPV devices. Nevertheless, Fig. S2 shows that with the morphological engineering of pentacene on the sub-cell, the ICL could be successfully formed, uniformly and without defects. Thus, the planar ICL was successfully prepared for the tandem solar cells by the introduction of pentacene.

Based on the valuable findings, we proceeded to fabricate planar tandem OPV cells under the high temperature annealing at 160 °C. Fig. 7 shows the *J–V* characteristics of single and tandem devices, while Tables 1 and 2 show the photovoltaic performance of single cells and tandem OPV devices, respectively. With morphology engineering using the pentacene, the bottom sub-cell for tandem organic solar cells was in planar morphology and beneficial to the ICL without any defects from crystallization of PCBM. The pentacene engineered tandem OPV devices showed an average PCE of 3.54% (J_{SC} of 4.79 mA/cm^2, V_{OC} of 1.18 V, and FF of 0.63). The performance of the tandem OPV showed an increase of 10% in PCE, compared with the best PCE of 3.20% from the single sub-cell of 130 nm.

Typically, with increasing thickness of the bottom sub-cell, the J_{SC} of the tandem device is supposed to be increased. However, the current matching in homo-tandem organic solar cells is complex. Fig. 2(c) shows that the highest PCE for a single sub-cell was 3.2% at the active layer thickness of 130 nm. The FF of the single sub-cell decreased when the active layer was too thick, but the J_{SC} is still increased. In Table 2 and Fig. S4(a) and (b) of the supplementary information, the highest PCE for tandem OPV devices is 3.54%, with the largest J_{SC} of 4.79 mA/cm^2, which is smaller than the J_{SC} of its bottom (single junction) sub-cell, of 5.94 mA/cm^2. However, the sum of J_{SC} from the two sub-cells of

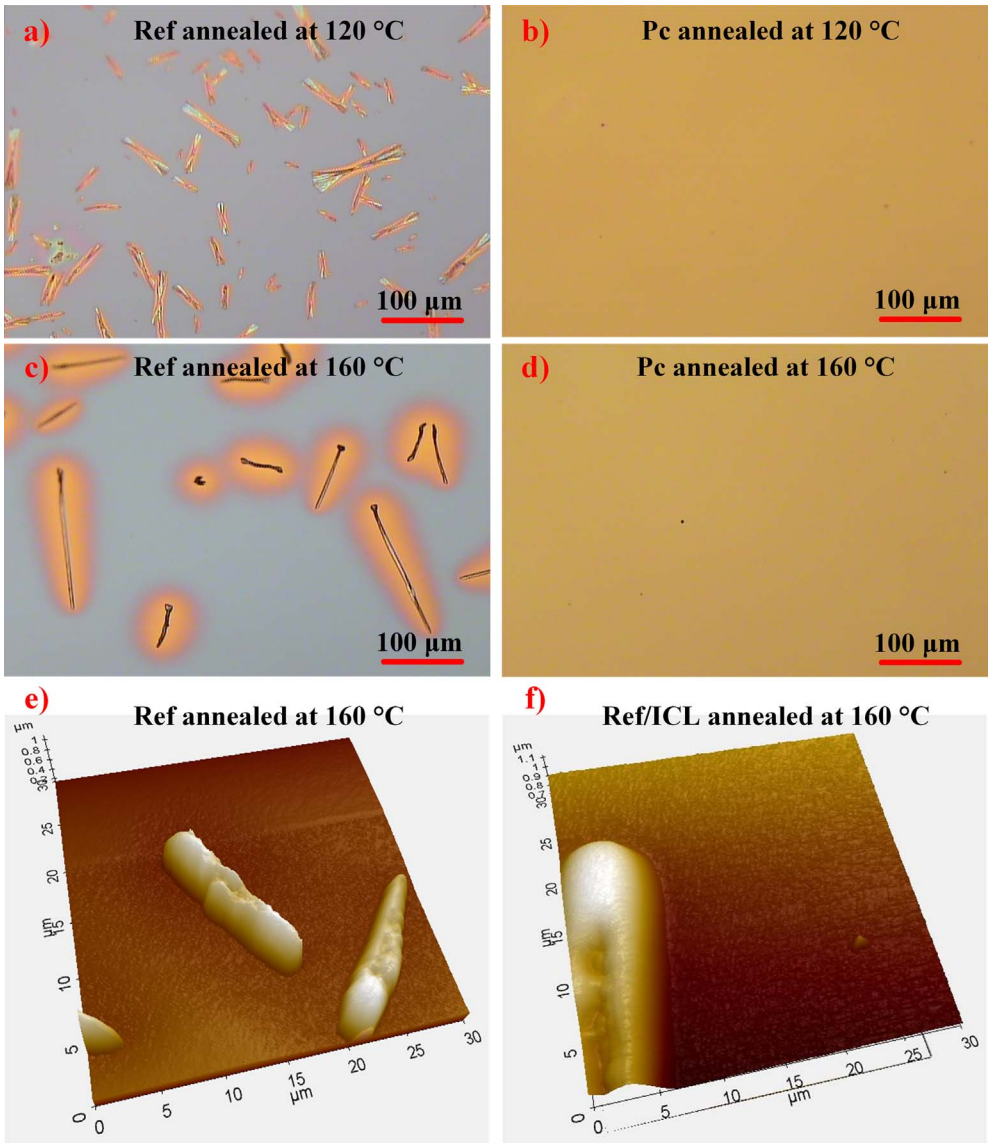

Fig. 6. Optical microscopy images of the active layers (a) P3HT:PCBM (Ref), and (b) P3HT:PCBM:Pentacene (Pc), annealed at 120 °C for 10 min; (c) P3HT:PCBM, and (d) P3HT:PCBM:Pentacene, annealed at 160 °C for 10 min. Scale bar = 100 μm. The AFM topography images of (e) P3HT:PCBM, and (f) interconnection layer (ICL) constructed on the active layer of P3HT:PCBM annealed at 160 °C for 10 min. The size of all AFM images is 30 μm × 30 μm.

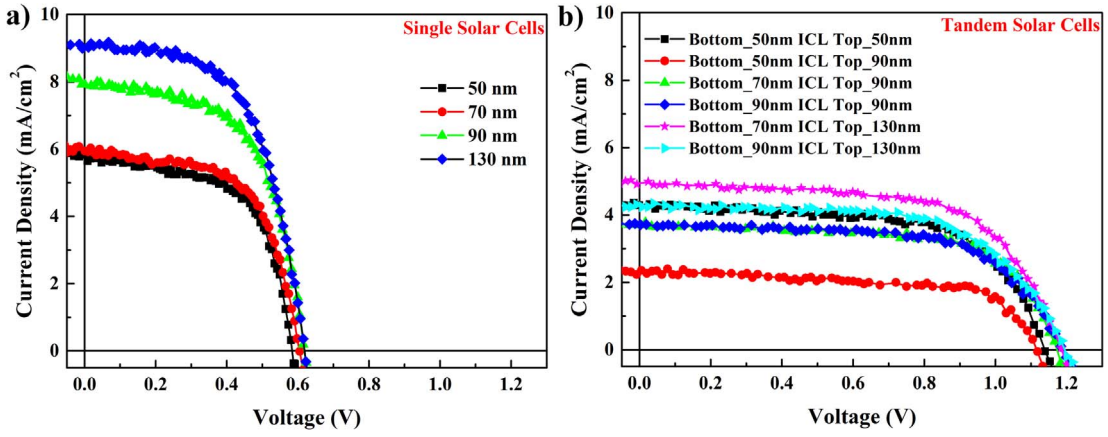

Fig. 7. Current density – voltage (*J–V*) characteristics of (a) single cells with different thickness active layers, and (b) tandem OPV devices with various thickness active layers of bottom and top sub-cells.

Table 1
Photovoltaic parameters of single cells with various thicknesses of active layer. The standard deviation is in brackets, and the average performance are from 6 devices.

Active layer thickness [nm]	J_{SC} [mA/cm^2]	V_{OC} [V]	FF	PCE [%]
50	5.75 (± 0.18)	0.58 (± 0.01)	0.60 (± 0.02)	2.02 (± 0.10)
70	5.94 (± 0.07)	0.61 (± 0.00)	0.60 (± 0.00)	2.17 (± 0.03)
90	7.91 (± 0.05)	0.61 (± 0.01)	0.58 (± 0.02)	2.78 (± 0.13)
130	8.98 (± 0.30)	0.62 (± 0.01)	0.58 (± 0.00)	3.20 (± 0.14)

homo-tandem device is 9.58 mA/cm^2, which is 7% enhancement compared to the best single junction solar cells. In addition, the FF of the two sub-cells increase 9% (from 0.58 to 0.63), which is due to their stronger hole and electron extraction in the thinner active layer of P3HT:PCBM. Although the V_{OC} of tandem solar device is a little lower than the sum of these of two single cells, there is only 4% lost in V_{OC}. As a result, the combined enhancement of J_{SC} and FF improves the PCE of tandem devices by 10%. The lost in J_{SC} of same thickness of active layer in single junction cell or sub-cells of tandem devices could be explained by the current balancing effect in homo-tandem organic solar cells.

Light management or current matching is very important for the design of high efficiency organic homo-tandem solar cells. Typically under the high temperature annealing at 160 °C, the PCBM crystals dramatically grow large, when the thickness of P3HT:PCBM active layer (without pentacene) increases from tens of nm (Yang et al., 2017a) to more than 100 nm (Yang et al., 2015). This is absolutely suppressed by the introduction of pentacene, so that the pentacene-assisted planar active layers of sub-cells for the tandem device could be applied with various thicknesses. In Fig. 8(a), the external quantum efficiency (EQE) in the range of 300–650 nm increases as the thickness of the active layer of the single device increases, whereas the transmittance (Fig. 8(b)) of the active layer dramatically decreases by about 30% as its thickness increases from 50 to 130 nm. Thus, the J_{SC} of the bottom sub-cell is shown to be very sensitive to the thickness of its active layer. In the tandem solar cells (Fig. 8(c), Fig. S3 of the supplementary information, and Table 2), the sun light (L1) only is a little absorbed once in the 50 nm bottom sub-cell and converted to a small photo-current, when the photo-active layer thickness of top sub-cell is 90 nm (strong absorption of sun light L2 and R2), which leads to a mismatched currents of the two sub-cells and a very small J_{SC} of 2.49 mA/cm^2 of tandem devices. With a 70 nm bottom sub-cell, the J_{SC} and PCE of the tandem cell are higher, because of its better current balance between the two sub-cells. The tandem solar cells with optimized bottom and top sub-cells (Fig. 8(c)) greatly increase their PCE (3.54%) by about 100%, comparing their highest PCE (3.54%) to their lowest PCE (1.75%). The PCE (3.54%) of our tandem solar cells is much improved when compared with the PCE of ca. 3% from the recently published homo-tandem OPV based on P3HT:PCBM blends under 160 °C annealing (Yang et al., 2017a; Zhao et al., 2011). It is easy to imply that the pentacene-assist planarization for tandem organic solar cells will enhance their performance and speed up the industry application of organic photovoltaics, with various efficient and complementary light-absorption donor materials.

In order to improve the PCE of tandem solar cells, we applied a perovskite (PRV) top sub-cell on top of the pentacene-assist organic bottom sub-cells with planar ICL. The PRV solar cell using methylammonium lead triodide ($MAPbI_3$) was developed similarly as in our recent study (Yang et al., 2017b). The tandem solar cells were fabricated from organic bottom sub-cells and $MAPbI_3$ PRV top sub-cells. Fig. 9(a) shows the UV–vis absorption of the photo-active layers of organic solar cells and $MAPbI_3$ PRV solar cells. The absorption range of organic P3HT:PCBM is mainly from 300 to 620 nm. The absorption range of $MAPbI_3$ semiconductor is from 300 to 780 nm. The non-overlapped absorption of top perovskite sub-cell from organic bottom sub-cell is from 620 to 780 nm, which can contribute to better utilization of incident solar spectrum. The photovoltaic performance of the tandem solar cells was summarized in Table 2 and Fig. 9(b). The J_{SC} of the OPV-PRV tandem solar cells is 10.18 mA/cm^2, which is much improved from the homo-tandem organic solar cells, 4.79 mA/cm^2. The V_{OC} of the OPV-PRV tandem solar cell, 1.5 V, is almost the sum of the organic (0.62 V) and PRV (0.96 V) sub-cells. The PCE of OPV-PRV tandem solar cells was improved to 7.63%.

4. Conclusions and future work

In summary, we applied pentacene-assisted active layers for efficient tandem organic solar cells based on the P3HT:PCBM blends under multi-thermal treatment. The possible PCBM crystallization of the P3HT:PCBM active layer under the thermal treatment at 160 °C could be suppressed by the pentacene addition, which offered planar and defect-free morphology. This led to successful deposition of the planar ICL layer and top sub-cells for tandem devices under the high temperature annealing at 160 °C. The homo-tandem organic solar cells achieved an average PCE of 3.54%, with J_{SC} = 4.79 mA/cm^2, V_{OC} = 1.18 V, and FF = 0.63. In contrast, the best single-junction cells with 130 nm P3HT:PCBM film achieved an average PCE of 3.20%. The tandem solar cells bring an essential increase of 10% in the device performance. However, the PCE of the homo-tandem solar cells based on P3HT:PCBM system is still too small to a practical industrial application of organic photovoltaics. The tandem solar cells were further developed with complementary light-absorption organic bottom sub-cells and PRV top sub-cells, which have higher PCE of 7.63%. We anticipate that the pentacene-assist planarization for tandem organic solar cells demonstrates a practical way to design highly efficient tandem organic solar cells against thermal treatments with various complementary light-absorption photo-active layers, which would greatly improve PCE of tandem organic photovoltaic devices.

Conflict of interest

There are no conflicts of interest to declare.

Table 2
Photovoltaic parameters of tandem OPV devices with various thickness active layers of sub-cells. The standard deviation is in brackets and the average performance are from 6 devices.

Bottom [nm]	Top [nm]	J_{SC} [mA/cm^2]	V_{OC} [V]	FF	PCE [%]
50	50	4.22 (± 0.09)	1.13 (± 0.01)	0.64 (± 0.02)	3.05 (± 0.04)
50	90	2.49 (± 0.47)	1.12 (± 0.02)	0.63 (± 0.06)	1.75 (± 0.45)
70	90	3.75 (± 0.19)	1.17 (± 0.01)	0.66 (± 0.01)	2.88 (± 0.19)
90	90	3.72 (± 0.11)	1.19 (± 0.01)	0.63 (± 0.01)	2.80 (± 0.04)
70	130	4.79 (± 0.05)	1.18 (± 0.01)	0.63 (± 0.01)	3.54 (± 0.09)
90	130	4.21 (± 0.16)	1.20 (± 0.01)	0.62 (± 0.00)	3.14 (± 0.15)
130	400[a]	10.18 (± 0.23)	1.49 (± 0.05)	0.50 (± 0.03)	7.63 (± 0.32)

[a] Top sub-cells of tandem cells were $MAPbI_3$ perovskite solar cells.

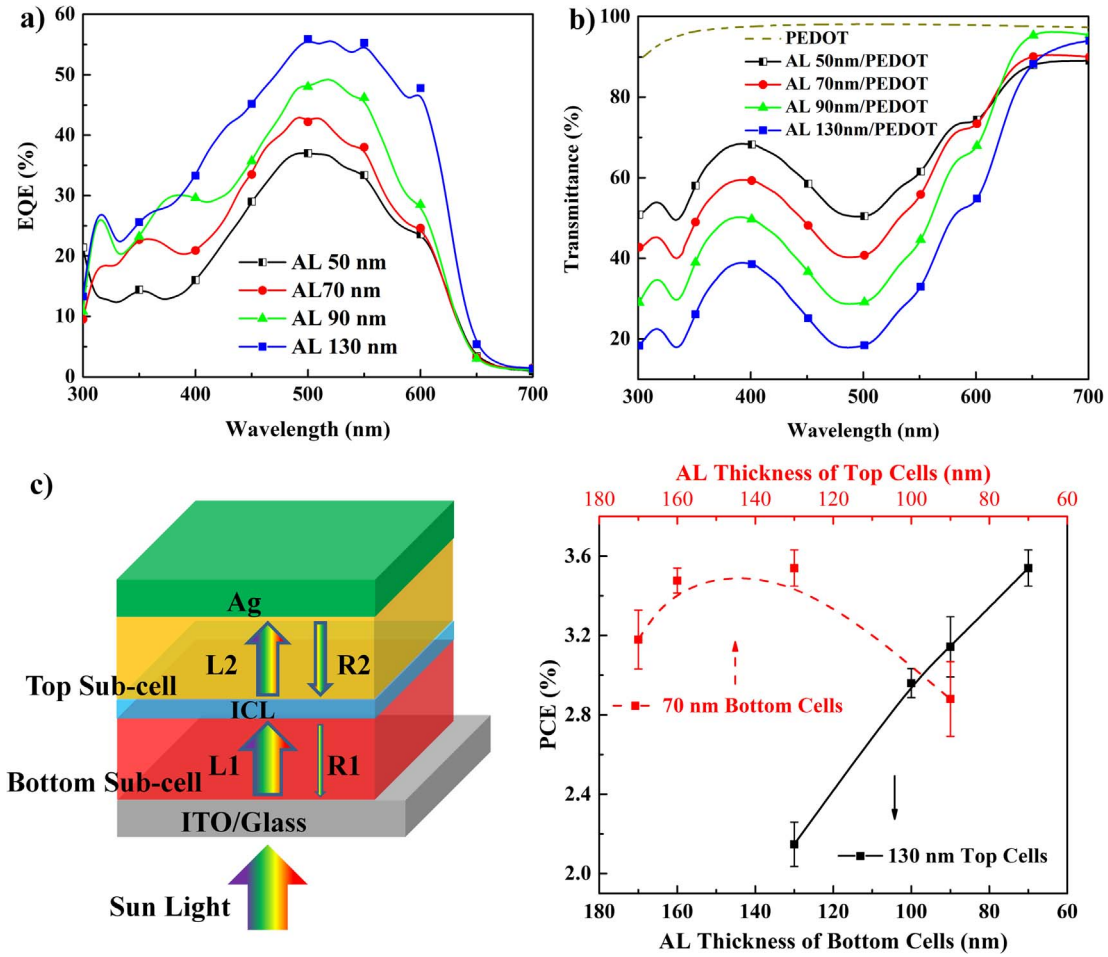

Fig. 8. The (a) EQE, and (b) transmittance of single sub-cells with various thickness active layer (AL). (c) The PCE of tandem OPV cells with various thickness of bottom (solid line) and top (dash line) sub-cells.

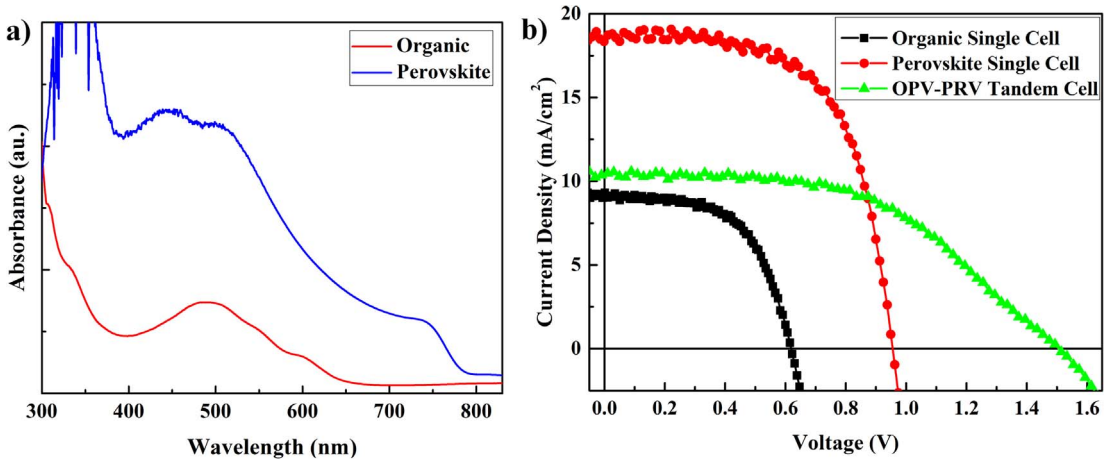

Fig. 9. (a) The UV–vis absorption of the photo-active layers of organic single cells and perovskite single cells. (b) Current density – voltage (*J–V*) characteristics of organic single cells (130 nm), perovskite single cells (400 nm), and tandem solar cells with organic bottom sub-cell (OPV) and perovskite top sub-cell (PRV).

Acknowledgments

This work was supported by Basic Science Research Program through the National Research Foundation of Korea (NRF) funded by the Ministry of Education [grant No. 2017R1D1A1B03033509].

Appendix A. Supplementary material

Figs. S1–S4, energy level diagram of the tandem OPV device, optical microscopy images of the interconnection layer (ICL), the sketch of light management for (a) single sub-cells and (b) tandem solar cells, and photovoltaic performance of various tandem OPV devices. Supplementary data associated with this article can be found, in the online version, at http://dx.doi.org/10.1016/j.solener.2018.01.093.

References

Akogwu, O., Akande, W., Tong, T., Soboyejo, W., 2011. Dendrite growth in annealed polymer blends for use in bulk heterojunction solar cells. J. Appl. Phys. 110 (10), 103517.

Ameri, T., Li, N., Brabec, C.J., 2013. Highly efficient organic tandem solar cells: a follow up review. Energy Environ. Sci. 6 (8), 2390–2413.

Ben Dkhil, S., Pfannmoller, M., Saba, M.I., Gaceur, M., Heidari, H., Videlot-Ackermann, C., Margeat, O., Guerrero, A., Bisquert, J., Garcia-Belmonte, G., Mattoni, A., Bals, S., Ackermann, J., 2017. Toward high-temperature stability of PTB7-based bulk heterojunction solar cells: impact of fullerene size and solvent additive. Adv. Energy Mater. 7 (4), 1601486.

Berriman, G.A., Holmes, N.P., Holdsworth, J.L., Zhou, X., Belcher, W.J., Dastoor, P.C., 2016. A new model for PCBM phase segregation in P3HT:PCBM blends. Org. Electron. 30, 12–17.

Busireddy, M.R., Mantena, V.N.R., Chereddy, N.R., Shanigaram, B., Kotamarthi, B., Biswas, S., Sharma, G.D., Vaidya, J.R., 2016. A dithieno 3,2-b:2′,3′-d pyrrole based, NIR absorbing, solution processable, small molecule donor for efficient bulk heterojunction solar cells. PCCP 18 (47), 32096–32106.

Chen, C.-C., Bae, S.-H., Chang, W.-H., Hong, Z., Li, G., Chen, Q., Zhou, H., Yang, Y., 2015. Perovskite/polymer monolithic hybrid tandem solar cells utilizing a low-temperature, full solution process. Mater. Horizons 2 (2), 203–211.

Chen, C.-C., Chang, W.-H., Yoshimura, K., Ohya, K., You, J., Gao, J., Hong, Z., Yang, Y., 2014. An efficient triple-junction polymer solar cell having a power conversion efficiency exceeding 11%. Adv. Mater. 26 (32), 5670–5677.

Chen, S.S., Zhang, G.Y., Liu, J., Yao, H.T., Zhang, J.Q., Ma, T.X., Li, Z.K., Yan, H., 2017. An all-solution processed recombination layer with mild post-treatment enabling efficient homo-tandem non-fullerene organic solar cells. Adv. Mater. 29 (6), 1604231.

Chen, Y.-L., Kao, W.-S., Tsai, C.-E., Lai, Y.-Y., Cheng, Y.-J., Hsu, C.-S., 2013. A new ladder-type benzodi(cyclopentadithiophene)-based donor-acceptor polymer and a modified hole-collecting PEDOT:PSS layer to achieve tandem solar cells with an open-circuit voltage of 1.62 V. Chem. Commun. 49 (70), 7702–7704.

Cheng, P., Yan, C., Wu, Y., Wang, J., Qin, M., An, Q., Cao, J., Huo, L., Zhang, F., Ding, L., Sun, Y., Ma, W., Zhan, X., 2016. Alloy acceptor: superior alternative to PCBM toward efficient and stable organic solar cells. Adv. Mater. 28 (36), 8021–8028.

Cui, Y., Yao, H., Gao, B., Qin, Y., Zhang, S., Yang, B., He, C., Xu, B., Hou, J., 2017. Fine-tuned photoactive and interconnection layers for achieving over 13% efficiency in a fullerene-free tandem organic solar cell. J. Am. Chem. Soc. 139 (21), 7302–7309.

Dou, L., You, J., Yang, J., Chen, C.-C., He, Y., Murase, S., Moriarty, T., Emery, K., Li, G., Yang, Y., 2012. Tandem polymer solar cells featuring a spectrally matched low-bandgap polymer. Nat. Photonics 6 (3), 180–185.

Etxebarria, I., Ajuria, J., Pacios, R., 2015. Solution-processable polymeric solar cells: a review on materials, strategies and cell architectures to overcome 10%. Org. Electron. 19, 34–60.

Grant, T.M., Gorisse, T., Dautel, O., Wantz, G., Lessard, B.H., 2017. Multifunctional ternary additive in bulk heterojunction OPV: increased device performance and stability. J. Mater. Chem. A 5 (4), 1581–1587.

Hsieh, C.-H., Cheng, Y.-J., Li, P.-J., Chen, C.-H., Dubosc, M., Liang, R.-M., Hsu, C.-S., 2010. Highly efficient and stable inverted polymer solar cells integrated with a cross-linked fullerene material as an interlayer. J. Am. Chem. Soc. 132 (13), 4887–4893.

Jørgensen, M., Norrman, K., Gevorgyan, S.A., Tromholt, T., Andreasen, B., Krebs, F.C., 2012. Stability of polymer solar cells. Adv. Mater. 24 (5), 580–612.

Kim, H.J., Han, A.R., Cho, C.-H., Kang, H., Cho, H.-H., Lee, M.Y., Fréchet, J.M.J., Oh, J.H., Kim, B.J., 2012. Solvent-resistant organic transistors and thermally stable organic photovoltaics based on cross-linkable conjugated polymers. Chem. Mater. 24 (1), 215–221.

Kong, J., Lee, J., Kim, G., Kang, H., Choi, Y., Lee, K., 2012. Building mechanism for a high open-circuit voltage in an all-solution-processed tandem polymer solar cell. PCCP 14 (30), 10547–10555.

Kouijzer, S., Esiner, S., Frijters, C.H., Turbiez, M., Wienk, M.M., Janssen, R.A.J., 2012. Efficient inverted tandem polymer solar cells with a solution-processed recombination layer. Adv. Energy Mater. 2 (8), 945–949.

Li, M.M., Gao, K., Wan, X.J., Zhang, Q., Kan, B., Xia, R.X., Liu, F., Yang, X., Feng, H.R., Ni, W., Wang, Y.C., Peng, J.J., Zhang, H.T., Liang, Z.Q., Yip, H.L., Peng, X.B., Cao, Y., Chen, Y.S., 2017. Solution-processed organic tandem solar cells with power conversion efficiencies > 12%. Nat. Photonics 11 (2), 85–90.

Li, S., Liu, W., Shi, M., Mai, J., Lau, T.-K., Wan, J., Lu, X., Li, C.-Z., Chen, H., 2016. A spirobifluorene and diketopyrrolopyrrole moieties based non-fullerene acceptor for efficient and thermally stable polymer solar cells with high open-circuit voltage. Energy Environ. Sci. 9 (2), 604–610.

Lu, S., Guan, X., Li, X., Liu, J., Huang, F., Choy, W.C.H., 2016. The incorporation of thermionic emission and work function tuning layer into intermediate connecting layer for high performance tandem organic solar cells. Nano Energy 21 (Suppl. C), 123–132.

Lu, S., Guan, X., Li, X., Sha, W.E.I., Xie, F., Liu, H., Wang, J., Huang, F., Choy, W.C.H., 2015. A new interconnecting layer of metal oxide/dipole layer/metal oxide for efficient tandem organic solar cells. Adv. Energy Mater. 5 (17), 1500631.

Mon, D., Higgins, A.M., James, D., Hampton, M., Macdonald, J.E., Ward, M.B., Gutfreund, P., Lilliu, S., Rawle, J., 2015. Bimodal crystallization at polymer-fullerene interfaces. PCCP 17 (3), 2216–2227.

Ouyang, X., Peng, R., Ai, L., Zhang, X., Ge, Z., 2015. Efficient polymer solar cells employing a non-conjugated small-molecule electrolyte. Nat. Photonics 9 (8), 520–524.

Proudian, A.P., Jaskot, M.B., Lyiza, C., Diercks, D.R., Gorman, B.P., Zimmerman, J.D., 2016. Effect of diels-alder reaction in C-60-tetracene photovoltaic devices. Nano Lett. 16 (10), 6086–6091.

Rabady, R.I., Manasreh, H., 2017. Thicknesses optimization of two- and three-junction photovoltaic cells with matched currents and matched lattice constants. Sol. Energy 158 (Suppl. C), 20–27.

Salim, T., Lee, H.-W., Wong, L.H., Oh, J.H., Bao, Z., Lam, Y.M., 2016. Semiconducting carbon nanotubes for improved efficiency and thermal stability of polymer-fullerene solar cells. Adv. Funct. Mater. 26 (1), 51–65.

Wang, J.L., Liu, K.K., Yan, J., Wu, Z., Liu, F., Xiao, F., Chang, Z.F., Wu, H.B., Cao, Y., Russell, T.P., 2016. Series of multifluorine substituted oligomers for organic solar cells with efficiency over 9% and fill factor of 0.77 by combination thermal and solvent vapor annealing. J. Am. Chem. Soc. 138 (24), 7687–7697.

Wang, K., Liu, C., Meng, T., Yi, C., Gong, X., 2016. Inverted organic photovoltaic cells. Chem. Soc. Rev. 45 (10), 2937–2975.

Wang, S.S., Qu, Y.P., Li, S.J., Ye, F., Chen, Z.B., Yang, X.N., 2015. Improved thermal stability of polymer solar cells by incorporating porphyrins. Adv. Funct. Mater. 25 (5), 748–757.

Watts, B., Belcher, W.J., Thomsen, L., Ade, H., Dastoor, P.C., 2009. A quantitative study of PCBM diffusion during annealing of P3HT:PCBM blend films. Macromolecules 42 (21), 8392–8397.

Yang, F., Kang, D.-W., Kim, Y.-S., 2017a. An efficient and thermally stable interconnecting layer for tandem organic solar cells. Sol. Energy 155, 552–560.

Yang, F., Kang, D.-W., Kim, Y.-S., 2017b. Improved interface of ZnO/$CH_3NH_3PbI_3$ by a dynamic spin-coating process for efficient perovskite solar cells. RSC Adv. 7 (31), 19030–19038.

Yang, F., Kim, J.-H., Ge, Z., Kim, Y.-S., 2015. Enhanced thermal stability of inverted polymer solar cells with pentacene. Isr. J. Chem. 55 (9), 1028–1033.

Yang, F., Park, E.-K., Kim, J.-H., Kim, Y.-S., 2016. Improved performance of inverted polymer solar cells using pentacene. Int. J. Energy Res. 40 (5), 677–684.

Yang, J., Zhu, R., Hong, Z., He, Y., Kumar, A., Li, Y., Yang, Y., 2011. A robust interconnecting layer for achieving high performance tandem polymer solar cells. Adv. Mater. 23 (30), 3465–3470.

You, J., Dou, L., Yoshimura, K., Kato, T., Ohya, K., Moriarty, T., Emery, K., Chen, C.-C., Gao, J., Li, G., Yang, Y., 2013. A polymer tandem solar cell with 10.6% power conversion efficiency. Nat. Commun. 4, 1446.

Zhang, K., Gao, K., Xia, R., Wu, Z., Sun, C., Cao, J., Qian, L., Li, W., Liu, S., Huang, F., Peng, X., Ding, L., Yip, H.-L., Cao, Y., 2016. High-performance polymer tandem solar cells employing a new n-type conjugated polymer as an interconnecting layer. Adv. Mater. 28 (24), 4817–4823.

Zhang, Q., Wan, X., Liu, F., Kan, B., Li, M., Feng, H., Zhang, H., Russell, T.P., Chen, Y., 2016. Evaluation of small molecules as front cell donor materials for high-efficiency tandem solar cells. Adv. Mater. 28 (32), 7008–7012.

Zhao, D.W., Ke, L., Li, Y., Tan, S.T., Kyaw, A.K.K., Demir, H.V., Sun, X.W., Carroll, D.L., Lo, G.Q., Kwong, D.L., 2011. Optimization of inverted tandem organic solar cells. Sol. Energy Mater. Sol. Cells 95 (3), 921–926.

Zhou, H., Zhang, Y., Mai, C.-K., Collins, S.D., Bazan, G.C., Nguyen, T.-Q., Heeger, A.J., 2015. Polymer homo-tandem solar cells with best efficiency of 11.3%. Adv. Mater. 27 (10), 1767–1773.